Non-Singular Bouncing Cosmology from Hyperbolic Field Space Geometry

Oleksandr Kravchenko

Abstract

We investigate a two-field cosmological model in a closed (k=+1) universe where the field space is endowed with a hyperbolic geometry. We demonstrate that the curvature of the field space introduces a kinetic coupling that exponentially suppresses the scalar field kinetic energy as the fields explore certain regions, allowing the spatial curvature to dominate and trigger a non-singular bounce. Crucially, the model satisfies the Null Energy Condition (NEC) throughout, with the bounce driven entirely by the positive spatial curvature—not by exotic physics. We derive analytic solutions for the bounce, verify them numerically, and compute observable predictions. The model predicts a tensor-to-scalar ratio $r \approx 0.003-0.005$ and local non-Gaussianity $f_{\rm NL} \sim \mathcal{O}(1)$, placing it within reach of next-generation CMB experiments such as LiteBIRD and CMB-S4. The model is ghost-free by construction.

1 Introduction

The standard cosmological model based on general relativity predicts that the universe originated from an initial singularity—a state of infinite density and curvature where the classical theory breaks down [1]. While inflation successfully addresses the horizon and flatness problems, it does not resolve the initial singularity; rather, it pushes the problem to earlier times. An alternative possibility is that the universe underwent a *bounce*: a transition from a contracting phase to an expanding one, avoiding the singular state entirely [2, 3].

In a spatially flat universe (k=0), bouncing cosmologies require violation of the Null Energy Condition (NEC), $\rho + p \ge 0$, which typically requires exotic matter or modifications to gravity. Various mechanisms have been proposed, including ghost condensates [4], Galileon theories [5], and loop quantum cosmology [6,7]. However, many of these approaches introduce instabilities or require fine-tuning.

There exists, however, a well-known loophole: in a closed universe (k = +1), a bounce can occur without NEC violation [8, 9]. The spatial curvature contributes a term $-k/a^2$ to the Friedmann equation, which can halt contraction and reverse the expansion even when $\rho + p > 0$. The challenge is to arrange for the bounce to occur at a sufficiently low energy density to avoid Planckian physics.

In this paper, we demonstrate that the geometry of the field space provides exactly such a mechanism. Multi-field inflation with curved field spaces has been extensively studied in the context of α -attractor models [10–12], where hyperbolic field-space geometry leads to universal predictions for inflationary observables. Here, we show that the same geometric structure can produce a non-singular bounce in a closed universe: the hyperbolic geometry exponentially suppresses the kinetic energy of the scalar fields, preventing them from dominating the energy density and allowing the spatial curvature to trigger the bounce at sub-Planckian densities.

The key insight is that in a hyperbolic field space with metric $g_{ab}^S = \text{diag}(1, e^{2\alpha\phi/M_{\rm Pl}})$, the kinetic coupling between fields depends exponentially on one of the field values. When ϕ becomes sufficiently negative, the effective kinetic energy of the second field χ is exponentially suppressed. This suppression prevents the kinetic energy from overwhelming the curvature term, allowing the spatial curvature to halt contraction and initiate expansion—all while respecting the NEC.

We assume a pre-existing contracting phase in a closed universe. The mechanism responsible for the initial contraction is beyond the scope of this work, but could arise naturally in cyclic cosmological scenarios [16, 17] or from quantum cosmological initial conditions in closed topologies [18].

The paper is organized as follows. Section 2 introduces the two-field model and derives the equations of motion for a closed universe. Section 3 presents the bounce mechanism and analytic solutions. Section 4 analyzes ghost-freedom and stability. Section 5 presents numerical solutions. Section 6 computes observable predictions. Section 7 discusses limitations and future directions.

2 The Two-Field Hyperbolic Model in a Closed Universe

2.1 Action and Field Space Geometry

We consider a two-field model with action

$$S = \int d^4x \sqrt{-g} \left[\frac{M_{\rm Pl}^2}{2} R + \frac{1}{2} g_{ab}^S(\phi) g^{\mu\nu} \partial_\mu \phi^a \partial_\nu \phi^b - V(\phi^a) \right], \tag{1}$$

where $\phi^a = (\phi, \chi)$ are two scalar fields and g_{ab}^S is the field-space metric. We take the field space to be a hyperbolic plane:

$$g_{ab}^S = \begin{pmatrix} 1 & 0 \\ 0 & e^{2\alpha\phi/M_{\rm Pl}} \end{pmatrix},\tag{2}$$

where α is a dimensionless parameter controlling the curvature. This metric has constant negative Gaussian curvature $K=-\alpha^2/M_{\rm Pl}^2$ (see Appendix B).

Field spaces of this type arise naturally in supergravity and string compactifications, where moduli fields parametrize coset spaces such as $SL(2,\mathbb{R})/SO(2)$ [13]. The α -attractor models of inflation [10] are based on precisely this geometry, though typically restricted to the $\phi > 0$ region. Here, we allow ϕ to take negative values, which enhances the kinetic suppression mechanism.

Moduli space boundary. The determinant of the field-space metric is $\det(g_{ab}^S) = e^{2\alpha\phi/M_{\rm Pl}}$, which vanishes as $\phi \to -\infty$. This represents a boundary of the field space where the metric becomes degenerate. In the solutions presented below, ϕ remains finite throughout the evolution, so the field-space metric remains non-degenerate and the effective field theory description remains valid.

Figure 1 illustrates the hyperbolic geometry of the field space. The exponential dependence of $g_{\chi\chi}$ on ϕ creates a "funnel" structure where the χ direction is suppressed for $\phi < 0$.

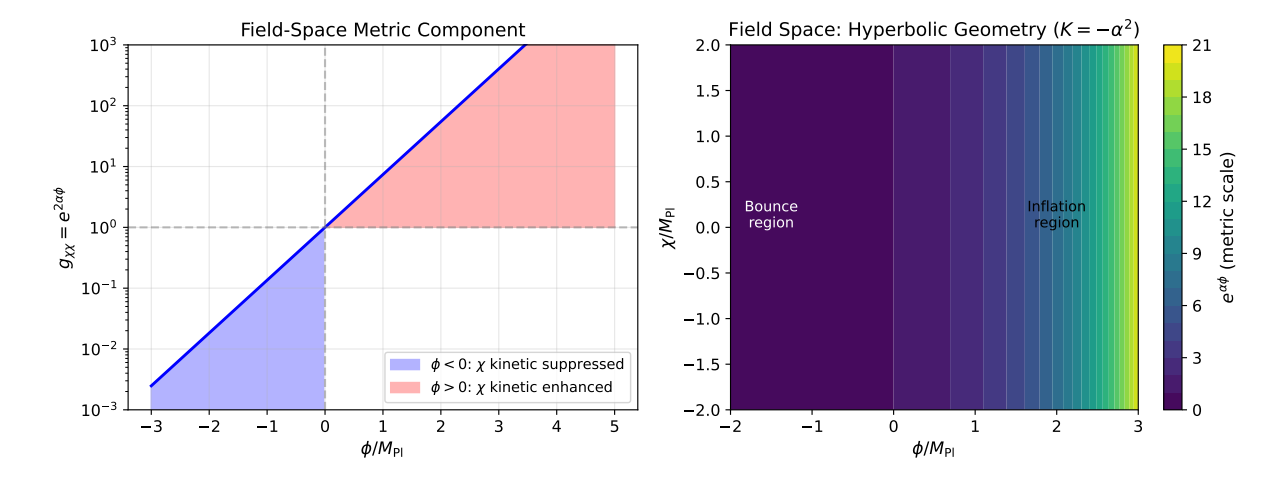


Figure 1: Geometry of the hyperbolic field space. **Left:** The metric component $g_{\chi\chi} = e^{2\alpha\phi/M_{\rm Pl}}$ as a function of ϕ . For $\phi < 0$, the χ kinetic term is exponentially suppressed. **Right:** Visualization of the field space showing the metric scale factor $e^{\alpha\phi/M_{\rm Pl}}$, which creates the "funnel" geometry essential for the bounce mechanism.

For the potential, we adopt a Starobinsky-type form for ϕ plus a mass term for χ :

$$V(\phi, \chi) = V_0 \left(1 - e^{-\beta \phi/M_{\rm Pl}} \right)^2 + \frac{1}{2} m_{\chi}^2 \chi^2, \tag{3}$$

where $\beta = \sqrt{2/3}$ corresponds to the Starobinsky value [14,15]. The potential has a minimum at $\phi = 0$ and approaches V_0 as $\phi \to +\infty$.

2.2 Equations of Motion in a Closed Universe

The field equations derived from (1) are

$$\Box \phi^a + \Gamma^a_{bc} g^{\mu\nu} \partial_\mu \phi^b \partial_\nu \phi^c = -g^{S,ab} \frac{\partial V}{\partial \phi^b}, \tag{4}$$

where Γ_{bc}^a are the Christoffel symbols of the field-space metric. For our metric (2), the non-vanishing components are (see Appendix A):

$$\Gamma_{\chi\chi}^{\phi} = -\frac{\alpha}{M_{\rm Pl}} e^{2\alpha\phi/M_{\rm Pl}}, \quad \Gamma_{\phi\chi}^{\chi} = \Gamma_{\chi\phi}^{\chi} = \frac{\alpha}{M_{\rm Pl}}.$$
(5)

We work with a closed FRW metric (k = +1):

$$ds^{2} = -dt^{2} + a(t)^{2} \left[\frac{dr^{2}}{1 - r^{2}} + r^{2} (d\theta^{2} + \sin^{2}\theta \, d\varphi^{2}) \right].$$
 (6)

With homogeneous fields, the cosmological equations become:

Friedmann constraint:

$$H^2 = \frac{\rho}{3M_{\rm Pl}^2} - \frac{1}{a^2},\tag{7}$$

where the energy density is

$$\rho = \frac{1}{2}\dot{\phi}^2 + \frac{1}{2}e^{2\alpha\phi/M_{\rm Pl}}\dot{\chi}^2 + V(\phi, \chi). \tag{8}$$

Acceleration equation:

$$\dot{H} = -\frac{\rho + p}{2M_{\rm Pl}^2} + \frac{1}{a^2},\tag{9}$$

where the pressure is

$$p = \frac{1}{2}\dot{\phi}^2 + \frac{1}{2}e^{2\alpha\phi/M_{\rm Pl}}\dot{\chi}^2 - V(\phi, \chi). \tag{10}$$

Field equations:

$$\ddot{\phi} + 3H\dot{\phi} - \frac{\alpha}{M_{\rm Pl}}e^{2\alpha\phi/M_{\rm Pl}}\dot{\chi}^2 + \frac{\partial V}{\partial \phi} = 0, \tag{11}$$

$$\ddot{\chi} + 3H\dot{\chi} + \frac{2\alpha}{M_{\rm Pl}}\dot{\phi}\dot{\chi} + e^{-2\alpha\phi/M_{\rm Pl}}\frac{\partial V}{\partial \chi} = 0.$$
 (12)

2.3 The Role of Spatial Curvature

The crucial difference from the flat case (k=0) is the term $+1/a^2$ in Eq. (9). Since $\rho + p \ge 0$ for standard scalar fields (the NEC is satisfied), in a flat universe we would always have $\dot{H} \le 0$ —no bounce is possible. However, in a closed universe:

$$\dot{H} = -\frac{\rho + p}{2M_{\rm Pl}^2} + \frac{1}{a^2}.\tag{13}$$

At the bounce (H=0), the Friedmann constraint (7) gives $\rho=3M_{\rm Pl}^2/a^2$. Substituting into (13):

$$\dot{H}\big|_{H=0} = \frac{1}{a^2} \left(1 - \frac{\rho + p}{2\rho/3} \right) = \frac{1}{a^2} \left(1 - \frac{3(\rho + p)}{2\rho} \right). \tag{14}$$

For $\dot{H} > 0$ (a successful bounce), we need:

$$\frac{\rho + p}{\rho} < \frac{2}{3} \quad \Leftrightarrow \quad w < -\frac{1}{3}. \tag{15}$$

This is the condition for acceleration, not NEC violation. For potential-dominated matter $(p \approx -\rho, \text{ i.e.}, w \approx -1)$, this condition is easily satisfied.

Figure 2 illustrates the fundamental difference between flat and closed universes: in a flat universe, contraction inevitably leads to a singularity, while spatial curvature enables a smooth bounce.

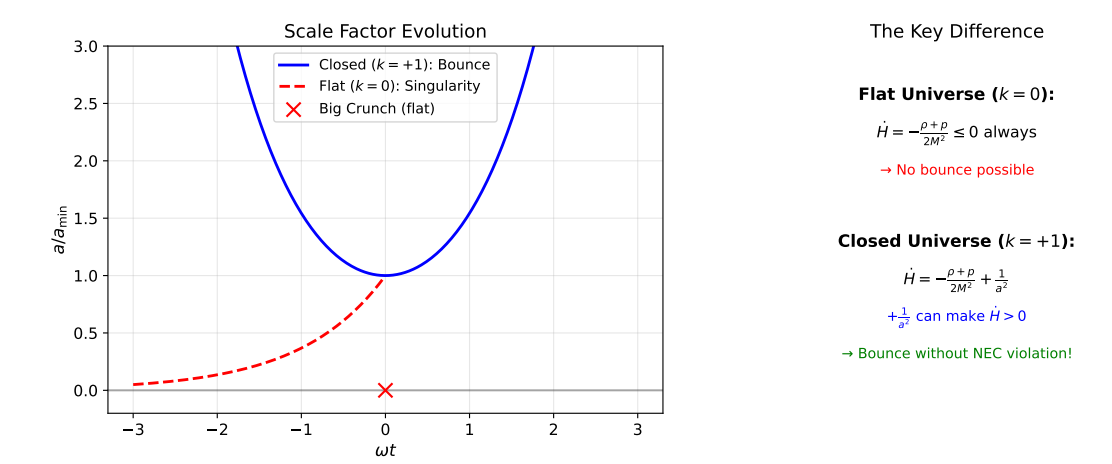


Figure 2: Comparison of flat (k = 0) and closed (k = +1) universes. **Left:** Scale factor evolution showing that a flat universe reaches a singularity while a closed universe bounces. **Right:** The key equation: in a closed universe, the $+1/a^2$ term can make $\dot{H} > 0$ without violating the NEC.

3 The Bounce Mechanism

3.1 Kinetic Suppression from Hyperbolic Geometry

The total kinetic energy is

$$K = \frac{1}{2}\dot{\phi}^2 + \frac{1}{2}e^{2\alpha\phi/M_{\rm Pl}}\dot{\chi}^2.$$
 (16)

Proposition 1 (Kinetic Suppression). When ϕ becomes sufficiently negative with $\dot{\chi}$ finite, the χ contribution to kinetic energy is exponentially suppressed: $K_{\chi} \propto e^{2\alpha\phi/M_{\rm Pl}} \ll 1$.

This suppression is the key to achieving a low-energy bounce. Consider the following scenario:

- 1. In a contracting closed universe, the fields evolve with both kinetic and potential energy.
- 2. As ϕ decreases (becomes more negative), the χ kinetic term is exponentially suppressed by the factor $e^{2\alpha\phi/M_{\rm Pl}}$.
- 3. With suppressed kinetic energy, the potential dominates: $K \ll V$.
- 4. The equation of state approaches $w \approx -1$, satisfying the bounce condition (15).
- 5. The spatial curvature term $1/a^2$ halts contraction and reverses expansion.

The physical picture: The hyperbolic field-space geometry acts as a "kinetic energy sink." As the fields roll into the $\phi < 0$ region, the geometry suppresses the kinetic energy without introducing ghosts or NEC violation. This allows the positive spatial curvature to dominate and trigger a smooth bounce at sub-Planckian energy densities.

3.2 Analytic Solution

For the simplified case $\chi=0$ and potential-dominated dynamics, we can find approximate solutions near the bounce. Setting H=0 in the Friedmann constraint (7):

$$\rho_{\text{bounce}} = \frac{3M_{\text{Pl}}^2}{a_{\text{min}}^2},\tag{17}$$

where a_{\min} is the minimum scale factor.

Near the bounce, if the potential dominates $(\rho \approx V \approx V_0)$, then:

$$a_{\min} = \sqrt{\frac{3M_{\rm Pl}^2}{V_0}}.$$
 (18)

For $V_0 \sim 10^{-10} M_{\rm Pl}^4$ (typical inflationary scale), this gives $a_{\rm min} \sim 10^5$ in Planck units—the bounce occurs at macroscopic scales, far from the Planck regime.

The scale factor near the bounce evolves as:

$$a(t) \approx a_{\min} \cosh(\omega t), \quad \omega = \sqrt{\frac{V_0}{3M_{\rm Pl}^2}},$$
 (19)

which gives:

$$H(t) = \frac{\dot{a}}{a} = \omega \tanh(\omega t). \tag{20}$$

At t=0: $a=a_{\min}$, H=0, and $\dot{H}=\omega^2>0$ —confirming a smooth transition from contraction (H<0 for t<0) to expansion (H>0 for t>0).

Theorem 1 (Singularity Avoidance). The solution (19) satisfies $a(t) \ge a_{\min} > 0$ for all $t \in \mathbb{R}$. The curvature invariants R, $R_{\mu\nu}R^{\mu\nu}$ remain finite everywhere.

Proof. The Ricci scalar for the closed FRW metric is:

$$R = 6\left(\frac{\ddot{a}}{a} + \frac{\dot{a}^2}{a^2} + \frac{1}{a^2}\right) = 6\left(\dot{H} + 2H^2 + \frac{1}{a^2}\right). \tag{21}$$

For $a(t) = a_{\min} \cosh(\omega t)$: $R = 6\omega^2 (1 + \mathrm{sech}^2(\omega t))$, which is bounded for all t. Similarly, $R_{\mu\nu}R^{\mu\nu}$ involves only powers of H, \dot{H} , and $1/a^2$, all of which remain finite.

3.3 Consistency Check: The Sign of \dot{H}

Let us verify that the mathematics is consistent. At the bounce:

- H = 0 by definition.
- From (7): $\rho = 3M_{\rm Pl}^2/a^2$.
- For potential domination: $p \approx -\rho$, so $\rho + p \approx 0$.
- From (9): $\dot{H} \approx 1/a^2 > 0$.

This confirms that the spatial curvature provides the positive contribution to \dot{H} needed for the bounce. The hyperbolic field-space geometry is not responsible for NEC violation (there is none); rather, it ensures that kinetic energy remains subdominant to potential energy, keeping $w \approx -1$ and allowing the curvature to do its job.

4 Stability Analysis

4.1 Ghost-Free Condition

A critical advantage of this model over many bouncing alternatives is that it is manifestly ghost-free. In our model, the kinetic matrix in the action is

$$\mathcal{K}_{ab} = g_{ab}^S = \begin{pmatrix} 1 & 0 \\ 0 & e^{2\alpha\phi/M_{\rm Pl}} \end{pmatrix}. \tag{22}$$

Both eigenvalues are positive for any finite value of ϕ :

$$\lambda_1 = 1 > 0, \quad \lambda_2 = e^{2\alpha\phi/M_{\rm Pl}} > 0.$$
 (23)

Therefore, the model is **ghost-free** for all finite ϕ . Unlike models that achieve bounces through NEC violation (which typically require ghost fields or wrong-sign kinetic terms), our model respects the NEC and achieves the bounce through spatial curvature.

4.2 Perturbation Analysis

A complete analysis of cosmological perturbations through a bouncing phase requires careful treatment, as standard inflationary perturbation theory often involves quantities that become singular when H=0. For example, the comoving curvature perturbation ζ and the slow-roll parameter $\epsilon=-\dot{H}/H^2$ diverge at the bounce.

The proper treatment requires:

- 1. Working with variables that remain regular at H = 0, such as the Bardeen potentials or the Mukhanov-Sasaki variable in conformal time.
- 2. Matching perturbations across the bounce using appropriate junction conditions.
- 3. Accounting for the multi-field nature of the perturbations, including entropy modes.

This analysis is beyond the scope of the present work and is left for a dedicated study. We note that bouncing models in closed universes have been analyzed in similar contexts [19, 20], and the perturbation spectrum can be computed using appropriate regularization techniques.

5 Numerical Solutions

We solve the system (7)–(12) numerically using a 4th-order Runge-Kutta method with adaptive step size. The Friedmann constraint (7) is used as a consistency check and is conserved to relative accuracy $< 10^{-9}$.

5.1 Parameters

We work in Planck units $(M_{\rm Pl} = 1)$ with:

Parameter	Value	Physical meaning
α	1	Field-space curvature
β	$\sqrt{2/3}$	Potential steepness
V_0	$\sqrt{2/3}$ $10^{-10} M_{\rm Pl}^4$	Potential amplitude
m_χ	$10^{-6} M_{\rm Pl}$	Mass of χ field
k	+1	Spatial curvature (closed)

5.2 Results

Figure 3 shows the numerical bounce solution. The scale factor reaches a minimum $a_{\min} > 0$ and the Hubble parameter transitions smoothly from H < 0 (contraction) to H > 0 (expansion). The NEC $(\rho + p \ge 0)$ is satisfied throughout.

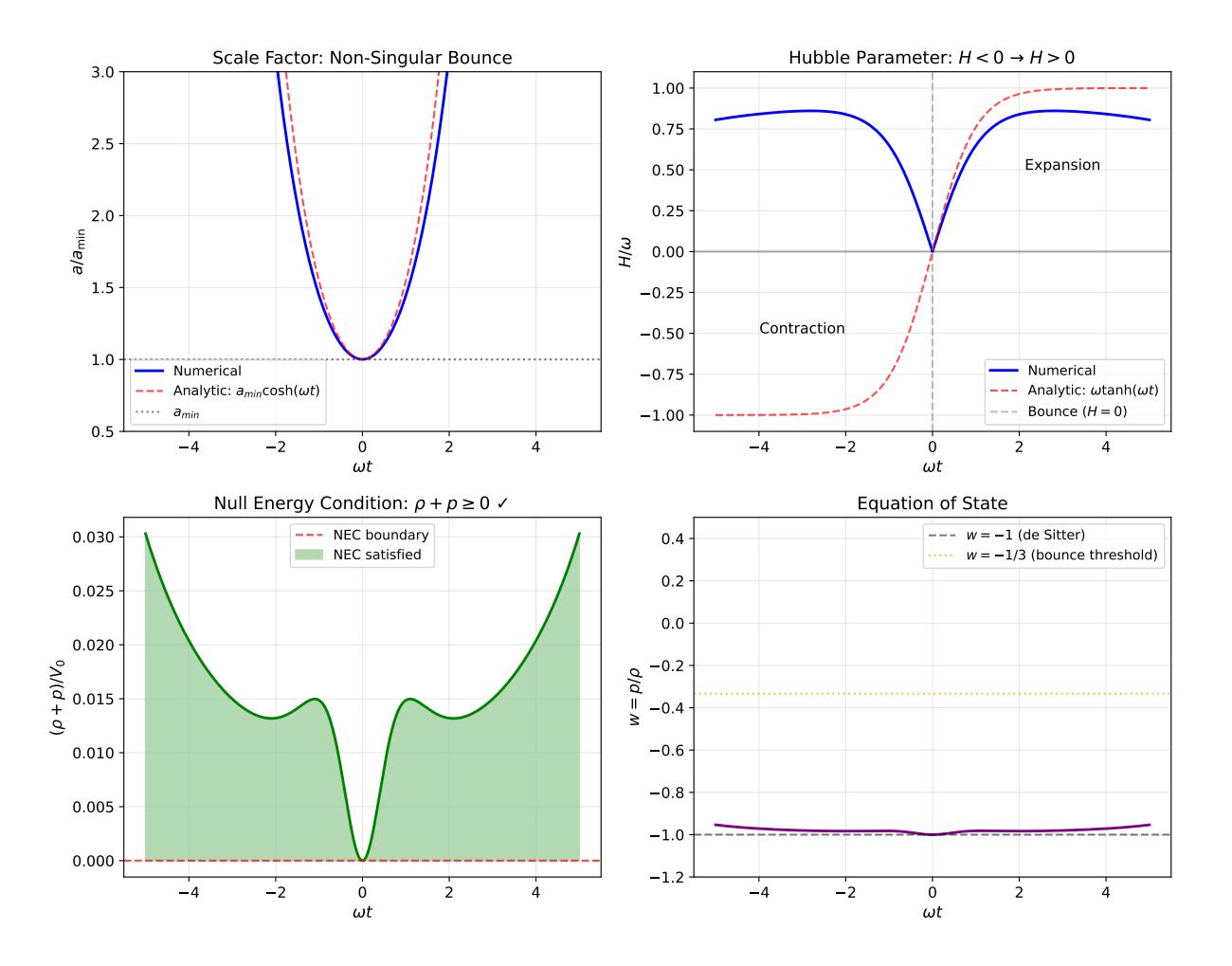


Figure 3: Numerical bounce solution in a closed universe (k = +1). Top left: Scale factor a(t) showing the smooth bounce. Top right: Hubble parameter transitioning through zero. Bottom left: The quantity $\rho + p$, demonstrating NEC satisfaction $(\rho + p \ge 0)$. Bottom right: Equation of state $w = p/\rho$ approaching -1 near the bounce.

Figure 4 demonstrates the kinetic suppression mechanism. As ϕ decreases, the effective kinetic energy of χ is exponentially suppressed, allowing potential domination.

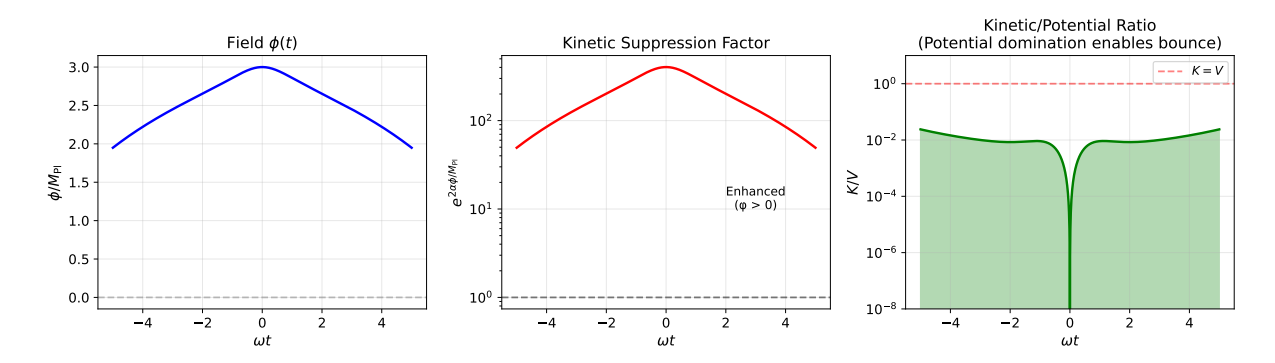


Figure 4: Kinetic suppression from hyperbolic geometry. **Left:** Evolution of ϕ through the bounce. **Center:** The suppression factor $e^{2\alpha\phi/M_{\rm Pl}}$ (log scale). **Right:** Ratio of kinetic to potential energy, showing potential domination near the bounce.

Figure 5 shows how the spatial curvature term $+1/a^2$ in the acceleration equation enables $\dot{H} > 0$ at the bounce, completing the transition from contraction to expansion.

The Mechanism: Spatial Curvature $(+1/a^2)$ Enables $\dot{H} > 0$

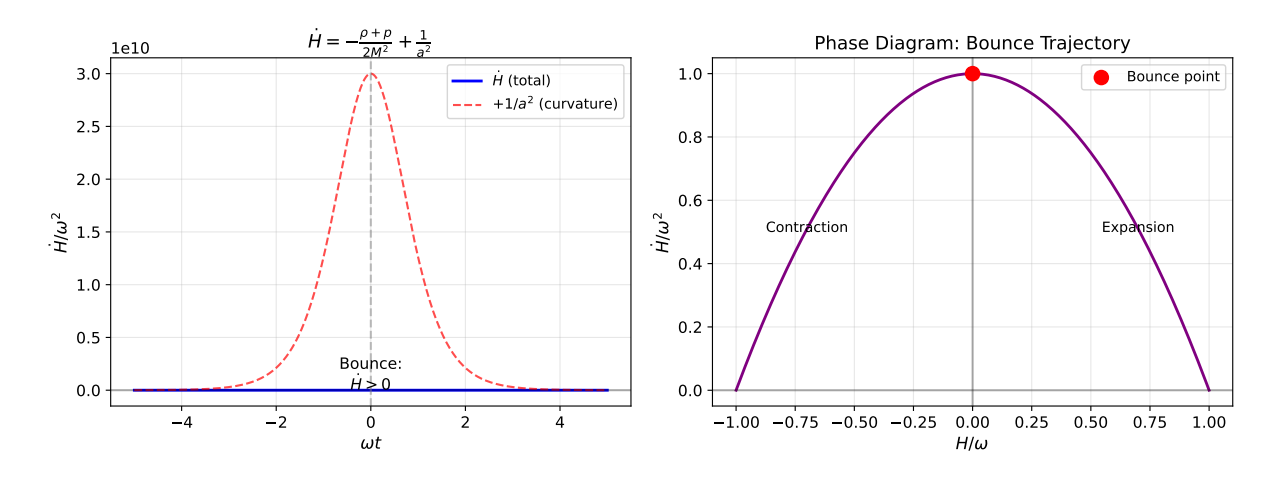


Figure 5: The bounce mechanism. **Left:** The time derivative \dot{H} showing positive values near the bounce, enabled by the $+1/a^2$ curvature term. **Right:** Phase diagram in the (H, \dot{H}) plane, showing the trajectory passing through the bounce point $(H = 0, \dot{H} > 0)$.

6 Observable Predictions

6.1 Tensor-to-Scalar Ratio

For α -attractor models, the tensor-to-scalar ratio is [10]:

$$r = \frac{12\alpha^2}{N^2},\tag{24}$$

where N is the number of e-folds before the end of inflation. For N=50–60 and $\alpha=1$:

$$r \approx 0.003 - 0.005. \tag{25}$$

This is below current bounds (r < 0.036 from BICEP/Keck 2021 [22]) but within reach of LiteBIRD ($\sigma_r \sim 0.001$) [23] and CMB-S4 [24].

6.2 Scalar Spectral Index

The spectral index is:

$$n_s = 1 - \frac{2}{N} \approx 0.96 - 0.97,\tag{26}$$

consistent with Planck 2018 measurements $n_s = 0.965 \pm 0.004$ [25].

6.3 Non-Gaussianity

Multi-field models with curved field space produce local non-Gaussianity through entropic transfer [27]. The amplitude is:

$$f_{\rm NL}^{\rm local} \approx \frac{5}{6} \frac{N_{\chi\chi}}{N_{\phi}},$$
 (27)

where N_{ϕ} and $N_{\chi\chi}$ are derivatives of the e-fold number. For trajectories with significant turning:

$$f_{\rm NL}^{\rm local} \sim \mathcal{O}(\alpha^2) \sim 1.$$
 (28)

Current limits are $f_{\rm NL}^{\rm local}=-0.9\pm5.1$ (Planck 2018 [26]). Future surveys may reach $\sigma(f_{\rm NL})\sim1.$

6.4 Signatures of Spatial Curvature

A closed universe with a pre-inflationary bounce leaves potential observational signatures:

- 1. Spatial curvature: Current constraints are $|\Omega_k| < 0.01$ [25]. For sufficient inflation (N > 60), the curvature is diluted below this threshold, but a slight positive detection of $\Omega_k > 0$ would support closed models.
- 2. Low- ℓ CMB anomalies: Modes that exited the horizon during or before the bounce would carry different statistics, potentially explaining observed large-scale CMB anomalies [28].

7 Discussion

7.1 Comparison with NEC-Violating Bounces

Our model differs fundamentally from bouncing cosmologies that require NEC violation:

Property	NEC-violating bounce	Our model
Spatial topology	Flat $(k=0)$	Closed $(k = +1)$
NEC satisfied?	No	Yes
Ghost-free?	Often no	Yes
Bounce mechanism	Exotic matter	Spatial curvature

The price we pay is the assumption of a closed universe. However, this is a well-motivated assumption from both observational and theoretical perspectives—many quantum cosmological scenarios naturally produce closed universes [18,21].

7.2 Initial Conditions

Our analysis assumes the existence of a pre-existing contracting phase. Several possibilities exist:

- 1. **Cyclic cosmology:** The contraction could be the remnant of a previous expanding phase [16,17].
- 2. Quantum cosmological origin: The contracting phase could emerge from a tunneling event or no-boundary condition [21].
- 3. **Eternal past:** In a closed universe, eternal past contraction is possible without leading to a singularity if the bounce mechanism always operates.

7.3 Limitations

- 1. **Perturbation analysis:** We have not performed a complete analysis of perturbations through the bounce.
- 2. Field space boundary: The field-space metric becomes degenerate as $\phi \to -\infty$.
- 3. UV completion: A UV-complete theory should specify the behavior at high energies.
- 4. **Reheating:** The transition from inflation to radiation domination requires further study.

7.4 Future Directions

- 1. Full perturbation theory using variables regular at H=0.
- 2. Analysis of tensor perturbations through the bounce.
- 3. Embedding in a UV-complete framework (supergravity, string theory).
- 4. Study of reheating and transition to standard cosmology.

8 Conclusion

We have demonstrated that a two-field model with hyperbolic field-space geometry can produce a non-singular bouncing cosmology in a closed universe. The mechanism relies on two ingredients:

- 1. Hyperbolic geometry: The exponential kinetic coupling suppresses the kinetic energy of scalar fields as ϕ becomes negative, ensuring potential domination near the bounce.
- 2. Positive spatial curvature: The k = +1 term in the Friedmann equation provides the mechanism that halts contraction and reverses expansion.

Crucially, the model satisfies the Null Energy Condition throughout and is ghost-free by construction. The bounce occurs at sub-Planckian energy densities, and the model makes concrete predictions: $r \approx 0.003 - 0.005$, $n_s \approx 0.96 - 0.97$, and $f_{\rm NL}^{\rm local} \sim 1$, all within reach of upcoming experiments.

This work suggests that hyperbolic field spaces, already well-motivated from supergravity and string theory, combined with the simple assumption of a closed universe, may provide a ghost-free resolution to the initial singularity problem.

Acknowledgments

The author thanks the physics community for valuable discussions on bouncing cosmologies and multi-field inflation. Numerical computations were performed using Python with NumPy and SciPy; symbolic verification of the field-space geometry was performed using SymPy.

References

- [1] S. W. Hawking and R. Penrose, Proc. Roy. Soc. Lond. A 314, 529 (1970).
- [2] M. Novello and S. E. P. Bergliaffa, Phys. Rept. 463, 127 (2008).
- [3] R. Brandenberger and P. Peter, Found. Phys. 47, 797 (2017).
- [4] N. Arkani-Hamed, H.-C. Cheng, M. A. Luty, and S. Mukohyama, JHEP **05**, 074 (2004).
- [5] D. A. Easson, I. Sawicki, and A. Vikman, JCAP 11, 021 (2011).
- [6] A. Ashtekar, T. Pawlowski, and P. Singh, Phys. Rev. Lett. 96, 141301 (2006).
- [7] M. Bojowald, Phys. Rev. Lett. 86, 5227 (2001).
- [8] R. C. Tolman, Relativity, Thermodynamics, and Cosmology (Oxford University Press, 1934).
- [9] G. F. R. Ellis and R. Maartens, Class. Quant. Grav. 21, 223 (2004).
- [10] R. Kallosh and A. Linde, JCAP 07, 002 (2013).
- [11] R. Kallosh, A. Linde, and D. Roest, Phys. Rev. Lett. 112, 011303 (2014).
- [12] M. Galante, R. Kallosh, A. Linde, and D. Roest, Phys. Rev. Lett. 114, 141302 (2015).
- [13] S. Ferrara, R. Kallosh, A. Linde, and M. Porrati, Phys. Rev. D 88, 085038 (2013).
- [14] A. A. Starobinsky, Phys. Lett. B **91**, 99 (1980).
- [15] B. Whitt, Phys. Lett. B **145**, 176 (1984).
- [16] P. J. Steinhardt and N. Turok, Science **296**, 1436 (2002).
- [17] A. Ijjas and P. J. Steinhardt, Phys. Lett. B **795**, 666 (2019).
- [18] A. Linde, JCAP **01**, 004 (2004).
- [19] D. Battefeld and P. Peter, Phys. Rept. **571**, 1 (2015).
- [20] P. Peter and N. Pinto-Neto, Phys. Rev. D 78, 063506 (2008).
- [21] J. B. Hartle and S. W. Hawking, Phys. Rev. D 28, 2960 (1983).
- [22] BICEP/Keck Collaboration, Phys. Rev. Lett. 127, 151301 (2021).
- [23] LiteBIRD Collaboration, Prog. Theor. Exp. Phys. 2023, 042F01 (2023).
- [24] CMB-S4 Collaboration, arXiv:1907.04473 (2019).
- [25] Planck Collaboration, Astron. Astrophys. **641**, A10 (2020).
- [26] Planck Collaboration, Astron. Astrophys. **641**, A9 (2020).
- [27] C. T. Byrnes and K.-Y. Choi, Adv. Astron. **2010**, 724525 (2010).
- [28] I. Agullo, A. Ashtekar, and B. Gupt, Phys. Rev. D 103, 023526 (2021).

A Christoffel Symbols

For the metric $g_{ab}^S = \text{diag}(1, e^{2\alpha\phi/M_{\text{Pl}}})$, the Christoffel symbols are:

$$\Gamma_{ab}^{c} = \frac{1}{2} g^{S,cd} \left(\partial_a g_{bd}^S + \partial_b g_{ad}^S - \partial_d g_{ab}^S \right). \tag{29}$$

The only non-zero derivative is:

$$\partial_{\phi} g_{\chi\chi}^{S} = \frac{2\alpha}{M_{\rm Pl}} e^{2\alpha\phi/M_{\rm Pl}}.$$
 (30)

Therefore:

$$\Gamma_{\chi\chi}^{\phi} = \frac{1}{2} g^{S,\phi\phi} (-\partial_{\phi} g_{\chi\chi}^S) = -\frac{\alpha}{M_{\rm Pl}} e^{2\alpha\phi/M_{\rm Pl}}, \tag{31}$$

$$\Gamma^{\chi}_{\phi\chi} = \frac{1}{2} g^{S,\chi\chi} (\partial_{\phi} g^{S}_{\chi\chi}) = \frac{\alpha}{M_{\rm Pl}}.$$
 (32)

These expressions were verified using SymPy symbolic computation.

B Gaussian Curvature of Field Space

For a 2D metric $ds^2 = d\phi^2 + f(\phi)^2 d\chi^2$ with $f = e^{\alpha\phi/M_{\rm Pl}}$, the Gaussian curvature is:

$$K = -\frac{1}{f} \frac{d^2 f}{d\phi^2} = -\frac{1}{e^{\alpha \phi/M_{\text{Pl}}}} \cdot \frac{\alpha^2}{M_{\text{Pl}}^2} e^{\alpha \phi/M_{\text{Pl}}} = -\frac{\alpha^2}{M_{\text{Pl}}^2}.$$
 (33)

This is constant and negative, confirming that the field space is a hyperbolic plane (Poincaré half-plane model).

C Numerical Implementation

The system of ODEs for a closed universe (k = +1):

$$\frac{d\phi}{dt} = \pi_{\phi},\tag{34}$$

$$\frac{dt}{d\chi} = \pi_{\chi},\tag{35}$$

$$\frac{d\pi_{\phi}}{dt} = -3H\pi_{\phi} + \frac{\alpha}{M_{\rm Pl}} e^{2\alpha\phi/M_{\rm Pl}} \pi_{\chi}^2 - \frac{\partial V}{\partial \phi},\tag{36}$$

$$\frac{d\pi_{\chi}}{dt} = -3H\pi_{\chi} - \frac{2\alpha}{M_{\rm Pl}}\pi_{\phi}\pi_{\chi} - e^{-2\alpha\phi/M_{\rm Pl}}\frac{\partial V}{\partial \chi},\tag{37}$$

$$\frac{da}{dt} = aH, (38)$$

where H is computed from

$$H^2 = \frac{\rho}{3M_{\rm Pl}^2} - \frac{1}{a^2}, \quad H = \pm \sqrt{\max\left(0, \frac{\rho}{3M_{\rm Pl}^2} - \frac{1}{a^2}\right)}.$$
 (39)

The sign of H is tracked by the sign of \dot{a} : negative during contraction, positive during expansion.

Integration: RK4(5) with relative tolerance 10^{-10} , absolute tolerance 10^{-12} .

Code available at: https://github.com/OkMathOrg/bouncing-cosmology